ACS Macro Letters

Letter

pubs.acs.org/macroletters

Atomistic Simulations Predict a Surprising Variety of Morphologies in Precise Ionomers

Dan S. Bolintineanu,* Mark J. Stevens, and Amalie L. Frischknecht*

Center for Integrated Nanotechnologies, Sandia National Laboratories, Albuquerque, New Mexico 87185, United States

Supporting Information

ABSTRACT: The nature of ionic aggregates in ionomers remains an important open question, particularly considering its significance to their unique electrical and mechanical properties. We have carried out fully atomistic molecular dynamics simulations of melts of lithium-neutralized precise ionomers that reveal the structural features of ionic aggregates in unprecedented detail. In particular, we observe a rich variety of aggregate morphologies depending on neutralization level and ionic content, including string-like and percolated aggregates. The traditional assumption of spherical ionic aggregates with liquid-like ordering that is typically used to interpret experimental scattering data is too simplistic; a more rich and complex set of structures exist that also fit the scattering data.

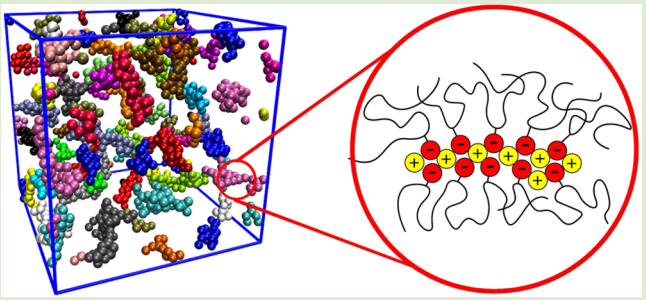

Ionomers are polymers that contain a small fraction of covalently bound ionic groups.[1] Due to various ionic interactions, ionomers exhibit unique electrical, thermal and mechanical properties. Applications of ionomers include semipermeable membranes, thermoplastic elastomers, resins for various packaging applications, and potentially solid electrolytes in batteries.[2] In a solvent-free ionomer melt, the low dielectric environment results in ionic aggregation, which has a significant impact on material properties. By controlling the ionic interactions (e.g., through polymer architecture, choice of cation/anion chemistries, extent of neutralization, temperature, etc.), material properties can in principle be finely tuned for the desired application.

In the present work, we focus on elucidating the ionic aggregate morphology in a series of recently synthesized linear poly(ethylene-*co*-acrylic acid) (PEAA) ionomers with precise spacing between acid groups.[3,4] Previously, we simulated precise ionomers using coarse-grained (CG) models[5−7] but were limited to treating full neutralization, because hydrogen bonding requires fine grained detail not present in the CG model. Here we investigate these systems using fully atomistic molecular dynamics simulations. This enables us to treat varying neutralization levels, to determine the atomic details of the ionic and hydrogen bonding interactions and to specifically treat Li ions. Unexpectedly, we find that ionic aggregate morphology varies strongly as a function of the neutralization level. While we confirm the stringy nature of the ionic aggregates found in the CG simulations, we find the aggregates range from isolated to percolated structures as a function of neutralization. In addition, aggregate formation relies on hydrogen bonds as well as ionic association. These atomistic simulations show that neutralization is a critical quantity and needs to be a focus of experimental work. The fundamental structure of the ionomer depends on neutralization, and this structure will strongly affect material properties such as conductivity.

Despite significant interest in ionic aggregate morphology, its investigation by traditional experimental techniques remains elusive. Relating X-ray or neutron scattering data to ionic aggregate morphology is difficult and typically relies on approximate analytical models. For instance, the strong ionomer peak at low wavevector found in virtually all ionomers, which is associated with interaggregate scattering, is often interpreted in terms of liquid-like hard-sphere scattering models.[8,9] However, using these models with confidence requires independent verification of these assumptions, for example by scanning transmission electron microscopy (STEM).[10−13] This has only been verified for a limited class of ionomer chemistries, not including PE-based ionomers, and only for spherical aggregate morphologies. Indeed, STEM cannot distinguish between projections of dense collections of spherical aggregates and those of string-like aggregates, and no direct evidence of string-like aggregates has emerged. In simulations, both aggregate morphologies and structure factors can be directly measured, and there is no need to rely on analytical scattering models and their associated assumptions.

The structures of the PEAA materials studied here are shown in Figure 1. In the present work, we study systems with spacer lengths of precisely 9, 15, and 21 carbons between carboxylic acid groups. We focus on lithium-neutralized systems due to the interest of the battery and fuel cell communities in this

Received: November 19, 2012
Accepted: February 11, 2013
Published: February 19, 2013

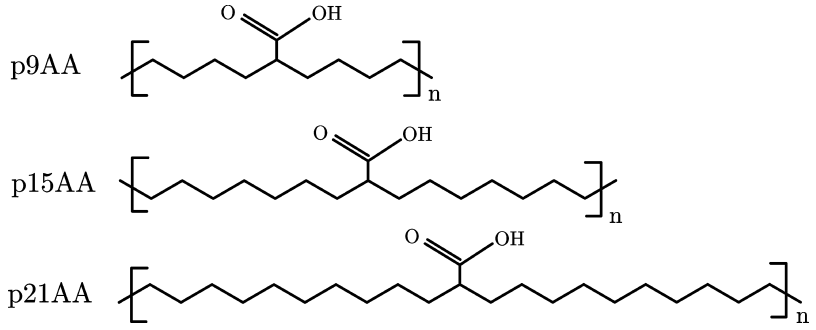

Figure 1. Chemical structures of the three polymers studied here. For the p9 copolymer, five different neutralization levels were simulated; for p15 and p21, only 43% neutralization levels were simulated.

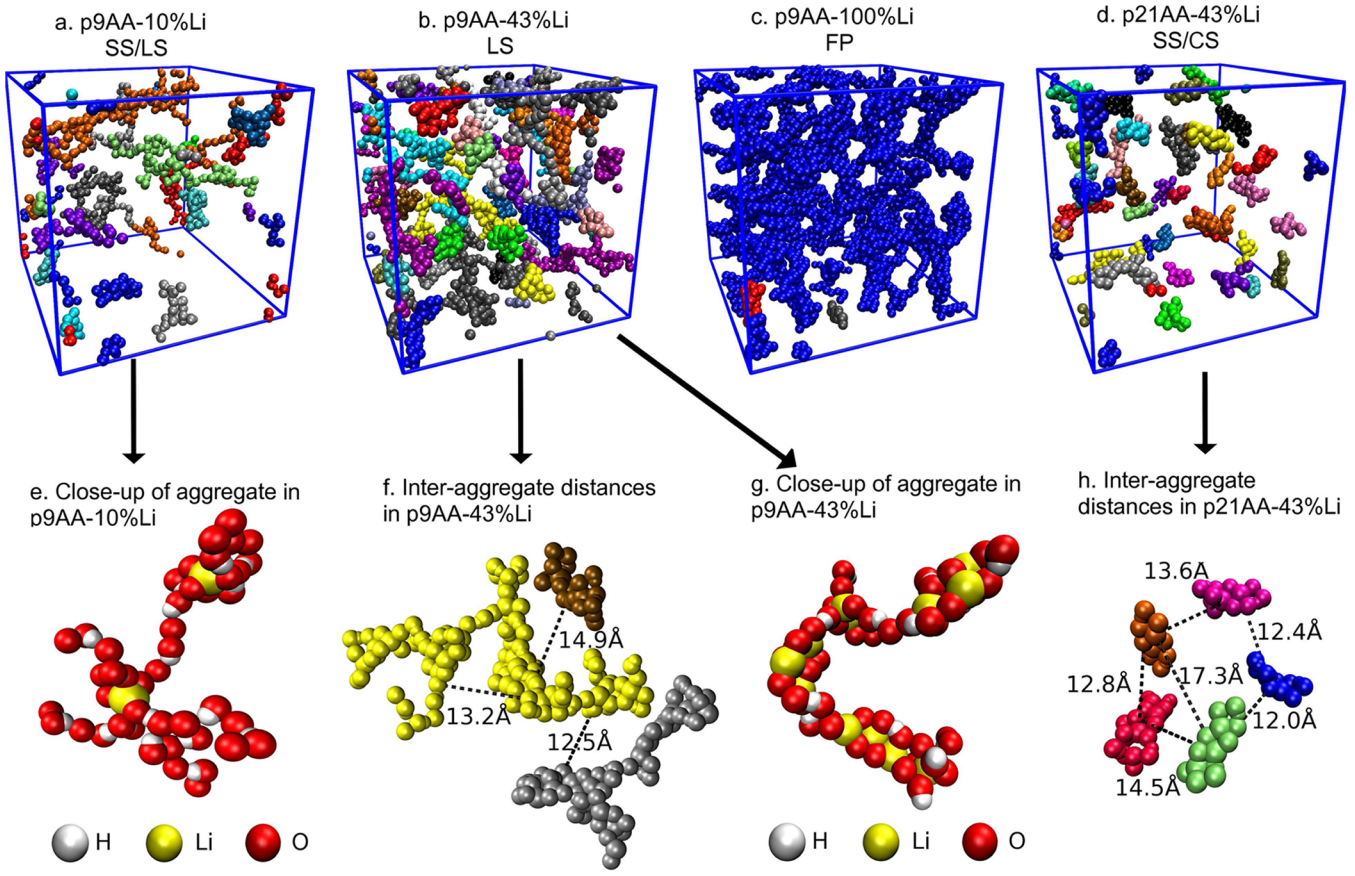

Figure 2. Visual representations of ionic aggregates. (a–d) Representative snapshots from simulations of several systems, where coloring is by aggregate. Only aggregates with two or more counterions are shown. (e, g) Close-up images of aggregates in p9AA-10%Li and p9AA-43%Li, respectively, showing lithium, oxygen and carboxyl hydrogen atoms. (f, h) Typical interaggregate distances in p9AA-43%Li and p21AA-43%Li, respectively.

cation. The nomenclature that we adopt lists the spacer length, the neutralization level, and the ion type: for example, p9AA-25%Li refers to a poly(ethylene-*co*-acrylic acid) polymer with a precise 9-carbon spacer, neutralized to 25% with lithium. Simulations were carried out for several neutralization levels for p9AA, as well as for all three spacer lengths at a fixed neutralization of 43%. All polymer chains contained four repeat units (n = 4), and all systems were simulated in cubic simulation boxes with side lengths of 60 to 65 Å. In all cases, the temperature was maintained at 150 °C, well above the glass transition temperature of these materials.[3,4]

In our simulations, we are able to directly visualize ionic aggregates. The definition and analysis of aggregates that we have employed are described in the Methods section. Figure 2 presents a visual summary of this analysis. In Figure 2a–d, we show snapshots from various systems, with distinct aggregates colored differently for ease of visualization. All lithium, oxygen, and carboxyl hydrogen atoms belonging to the same aggregate are drawn in the same color. Only aggregates containing two or more lithium counterions are shown. In most cases, more than 90% of lithium ions belong to such aggregates (the exception is p9AA-10%Li, where the fraction is 65%; see Table S1 in the Supporting Information). This matches recent MD simulations of poly(ethylene oxide)-based ionomers,[14] although strong differences are otherwise expected between PE and PEO-based polymers. Clearly, aggregate morphologies vary significantly

dx.doi.org/10.1021/mz300611n | *ACS Macro Lett.* 2013, 2, 206–210

among the systems and most bear little resemblance to the spherical shapes with liquid-like ordering typically assumed in scattering models. For the p9AA systems at low to moderate neutralization levels, stringy, branched aggregates are observed. At the lowest neutralization (10%), the density of strings is lower, and shorter segments can be seen; at 43% neutralization, the strings are much longer and often branch; as neutralization is increased further, the strings percolate throughout the simulation box. We distinguish two morphological regimes in the p9AA systems, consisting of long, stringy aggregates (LS) and fully percolated aggregates (FP), in which almost all the ions are in a single percolating cluster. These morphologies are consistent with recent coarse-grained simulations of analogous fully neutralized systems.[5,6] Two intermediate morphologies can also be defined, corresponding to short, stringy aggregates (SS) and partially percolated systems (PP), in which many aggregates exist that are not in the percolating cluster. The spacer length also has a significant effect on aggregate morphology. As seen in Figure 2d, the aggregates in p21AA-43%Li are notably smaller than in any other case, but even these do not fully resemble the spherical aggregates with liquid-like order that are traditionally assumed in interpreting scattering data. We denote this morphology as compact, isolated aggregates (CI). It is also worth noting that the change in morphology in this case is not due to net ion concentration alone; the ion concentration in the p21AA-43%Li system is 0.63 nm^{-3}, placing it between the p9AA-10%Li and p9AA-25% Li systems (with concentrations of 0.32 and 0.79 nm^{-3}, respectively). Because both of these systems show stringy aggregate morphologies, we can conclude that morphology in these systems is a function of both ion concentration and the relative abundance of neutralized and acidic sites. Aggregate morphologies are summarized in Table 1.

Table 1. Aggregate Morphology as a Function of Neutralization Level and Spacer Length[a]

	10%	25%	43%	75%	100%
p9	SS/LS	LS	LS	LS/PP	FP
p15			SS		
p21			SS/CI		

[a]Abbreviations are as follows: CI, compact, isolated; SS, short, stringy; LS, long, stringy; PP, partially percolated; FP, fully percolated. See text for further details.

We have computed the structure factor in order to directly compare to experimental scattering data. Figure 3 shows the total structure factor as a function of neutralization level for the lithium-neutralized p9AA systems. The ionomer peak at low q values is clearly seen in all cases, at $q \approx 4-6$ nm^{-1}. This peak corresponds to interaggregate scattering, where aggregates are typically assumed to be composed of high-contrast ionic species, in this case, counterions and acid/anionic groups. The amorphous halo, which extends from $q \approx 10$ to $q \approx 16$ nm^{-1}, arises from scattering among aliphatic chains and other short-range interactions. As expected, higher neutralization levels lead to an increase in the height of the ionomer peak relative to the amorphous halo, suggesting either an increase in the degree of aggregate ordering or a higher concentration of high-contrast ionic species in the aggregates. We also note a slight shift of the ionomer peak toward lower q with increasing neutralization. We explain this by noting that the addition of counterions leads to a sharp increase in the size of aggregates, rather than an

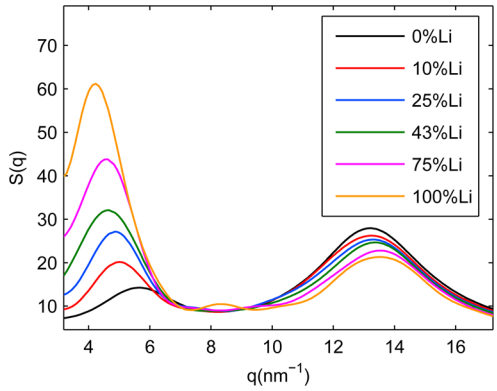

Figure 3. Structure factor as a function of neutralization level for lithium-neutralized p9AA.

increase in the number density of aggregates. The mean interaggregate distance thus increases, leading to slightly lower q values of the ionomer peak with higher neutralization. In p9AA-100%Li, the small peak near $q \approx 8$ nm^{-1} appears to correspond to intra-aggregate effects, most likely due to scattering among thicker segments belonging to the same aggregate. In partially neutralized systems, aggregate compositions are inherently heterogeneous (containing both acid groups and carboxylate anions), so that the order of these thicker segments is broken, and no such peak appears.

We have also investigated the effects of the spacer length on the structure factor, shown in figure 4. The ionomer peak shifts

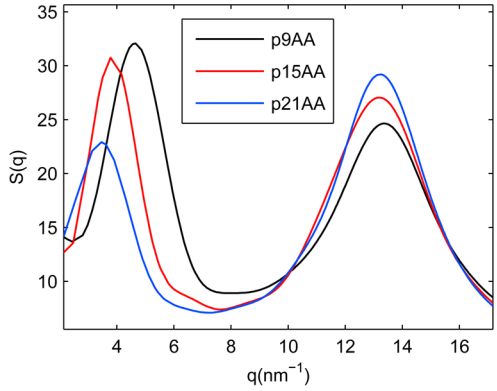

Figure 4. Structure factors for three spacer lengths at 43% neutralization.

to lower q values with higher spacer lengths. This suggests an increase in the interaggregate spacing, which is to be expected with a larger spacer, because this increases the spacing between ionic groups and therefore aggregates. The same trend in peak locations was observed experimentally for zinc- and sodium-neutralized systems[4,5] as well as in coarse-grained simulations.[5] Both the shape and location of the ionomer peak as well as the amorphous halo are in good agreement with experimental data available for similar systems: in the same materials neutralized with sodium, experiments show ionomer peaks that extend from $q \approx 3-5$ nm^{-1} for a p9AA-33%Na system and $q \approx 2.5-5.5$ nm^{-1} for a p15AA-34%Na system.[5] In both cases, the amorphous halo was found to extend from $q \approx 10$ nm^{-1} to just beyond the largest wavevector accessible ($q \approx 16$ nm^{-1}). In our simulations, the ionomer peak extends from $q \approx 2.5-7$ nm^{-1} in the p9AA-43%Li case and from $q \approx 2-6.5$ nm^{-1} in the p15AA-

dx.doi.org/10.1021/mz300611n | ACS Macro Lett. 2013, 2, 206−210

43%Li system; the amorphous halo in all cases extends from $q \approx 10-17$ nm^{-1}.

Although scattering spectra and simulation structure factors capture changes in characteristic length scales associated with ionic aggregates, interpreting these changes in terms of morphological features is difficult. In simulations, we are able to verify the real-space interaggregate distances and compare these to the q-values of the ionomer peak. In Figure 2f,h, several representative interaggregate distances are shown, ranging from 12 to 17 Å, which corresponds to $q \approx 3.6-5.2$ nm^{-1}. This is in excellent agreement with the location of the ionomer peak in the structure factor data (3−6 nm^{-1}), confirming that the ionomer peak is indeed a result of interaggregate scattering. In the case of stringy aggregates (Figure 2f), a unique measure of the interaggregate distance cannot easily be defined; the indicated labels correspond approximately to the minimum separation distances between nearest-neighbor aggregates (interaggregate distances that appear closer are an effect of the two-dimensional rendering). In the compact, isolated aggregate case of panel (h), interaggregate distances are much easier to define, and the labels correspond approximately to the center of mass separation among nearest-neighbor aggregates. In both cases, we have not attempted a more rigorous measurement of all interaggregate distances, as this information is effectively contained in the structure factor data; instead, the measurements shown are meant only to provide a visual and intuitive understanding of the origin of the ionomer peak and its relationship to aggregate morphology.

We have used the MD configurations to quantify several short-range interactions and their relationship to aggregate morphologies. More detail is given in the Supporting Information, along with radial distribution functions (rdfs) for several key atomic species near lithium ions. The rdfs reveal the expected lithium−oxygen−lithium packing motif, which is consistent with the aggregate image shown in Figure 2e,g, particularly for the case of p9AA-43%Li. Presumably, the steric hindrance from the polymer backbone near the oxygen atoms limits the growth of this packing motif to one dimension, which results in the string-like morphology. A schematic of a generic stringy aggregate is shown in Figure 5, which stands in contrast to the spherical core−shell models typically assumed.[8,9,15] Additionally, the presence of hydroxyl groups suggests that hydrogen-bonded networks play a secondary but important role in aggregate formation under certain conditions. For instance, in the case of p9AA-10%Li, the long stringy aggregates that are observed largely consist of hydrogen-bonded networks, as shown in Figure 2e. As the neutralization level is increased, the importance of hydrogen-bonding to aggregate growth diminishes. In the p9AA-43%Li case, hydrogen bonds occasionally connect lithium-rich domains of aggregates, resulting in longer strings than would otherwise occur (see Figure 2g). Our simulations are in good agreement with recent NMR experiments with regard to lithium coordination and experimentally measured lithium−hydrogen distances.[16]

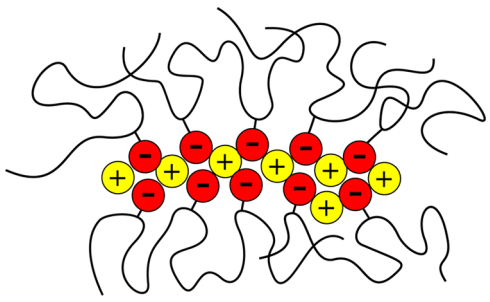

Figure 5. Schematic of stringy aggregate. The stringy geometry keeps cations from being in direct contact with one another, while steric hindrance in chain packing limits aggregate growth to one dimension.

In summary, we have carried out extensive molecular dynamics simulations for a set of precise ionomers neutralized with lithium, in which we varied neutralization and spacer length in order to compare directly to experiments. We observe significant changes in ionic aggregate morphology as a function of these parameters, despite apparent similarities in the structure factor data. In particular, increased neutralization leads to increasingly longer stringy aggregates, eventually leading to aggregates with percolated network structures (see Figure 2). Longer spacers between functional groups have the opposite effect, leading to shorter strings and eventually compact, isolated aggregate shapes. The atomistic simulations capture the effects of hydrogen bonding in these systems, which we have shown to be an important part of the aggregate formation mechanism. We are also able to explain the qualitative similarities in the ionomer peak location among experimental systems, despite vastly different aggregate morphologies: in the case of stringy morphologies, interaggregate distances, as measured approximately by the distance of closest approach between strings, correspond closely to center-to-center separations in compact, isolated morphologies. Overall, the picture that emerges stands in stark contrast to the spherical aggregates with liquid-like order that are often assumed in interpreting experimental scattering data.

METHODS

All systems with the precise 9-carbon (p9) spacer contained 200 polymer molecules, while the p15 and p21 copolymers contained 120 and 80 molecules, respectively. In all cases, all polymer molecules contained four repeat units. All simulations were carried out using the OPLS-AA fully atomistic force field, including explicit hydrogen atoms.[17] Lithium nonbonded parameters correspond to those given by Jensen and Jorgensen.[18] The LAMMPS software package was used for all simulations,[19] with a real-space nonbonded cutoff of 12 Å and the particle−particle particle-mesh solver for electrostatics.[20] A Langevin thermostat with a 100.0 fs damping parameter was used to maintain a constant temperature of 150 °C. The integration time step was set to 1.0 fs in all cases. All systems were constructed by placing polymer chains and free ions in random locations on a simple cubic lattice at a low density, and subsequently isotropically compressing the systems to a density of approximately 1 g/cm^3 during 0.5 ns. An additional 2 ns simulation was carried out at a constant pressure of 1 atm in the NPT ensemble to allow each system to reach its equilibrium density. The equilibrated dimensions of the cubic simulation boxes ranged from 60 to 65 Å per side. The box dimensions were subsequently fixed, and production runs were carried out in the NVT ensemble for approximately 30 ns for each system. We have verified the convergence of our simulations with a set of parallel tempering simulations and a longer MD simulation. Additionally, we have confirmed for several systems that different starting states lead to no significant differences in the structure factor data or the morphologies. A more detailed discussion is given in the Supporting Information.

Structure factors that account for atomic form factors were computed from Fourier transforms of the pairwise radial distribution functions, according to the following scheme:

$$S(q) = \sum_i c_i f_i^2 + 4\pi\rho \int_0^\infty \frac{\sin(qr)}{qr} r^2 \sum_{i,j} c_i c_j f_i f_j (g_{ij}(r) - 1)\mathrm{d}r \quad (1)$$

dx.doi.org/10.1021/mz300611n | ACS Macro Lett. 2013, 2, 206−210

Here, i and j are indices corresponding to distinct atomic species (lithium, oxygen, carbon, or hydrogen), g_{ij} is the radial distribution function between species i and j, ρ is the total number density of the system, c_i and f_i are the mole fraction and atomic scattering function for species i, respectively. The atomic scattering functions f_i are based on the empirical fits of Waasmaier and Kirfel,[21] which take the form $f_i = c_i + \sum_{k=1}^{5} a_{ik} \exp(-b_{ik} q_0^2))$, where a_{ik}, b_{ik}, and c_i are tabulated sets of coefficients for each atomic (ionic) species i.

The following definition of ionic aggregates was found to be most appropriate: (1) all lithium−oxygen pairs and oxygen−carboxyl hydrogen pairs that are within a certain cutoff distance of each other are considered to belong to the same aggregate; (2) all oxygens and carboxyl hydrogens that belong to the same carboxylate/carboxylic acid group are also considered to belong to the same aggregate. Both conditions are applied to all atoms in a pairwise search clustering algorithm. The cutoff distances for lithium−oxygen and oxygen−hydrogen pairs were found based on the atomic contact distance, which was defined to be the entirety of the first peak in the radial distribution function for a particular pairing. We include the oxygen−carboxyl hydrogen pairing because hydrogen-bonded networks form readily in these systems as a result of these interactions and have important effects on aggregate formation. An alternative aggregate definition and its effect on measured morphology is discussed in the Supporting Information.

■ ASSOCIATED CONTENT

Supporting Information

Verification of simulation convergence; effects of an alternate aggregate definition; and radial distribution functions. This material is available free of charge via the Internet at http://pubs.acs.org.

■ AUTHOR INFORMATION

Corresponding Author

*E-mail: dsbolin@sandia.gov; alfrisc@sandia.gov.

Notes

The authors declare no competing financial interest.

■ ACKNOWLEDGMENTS

We thank Prof. Karen Winey for many useful discussions and comments on the manuscript. We also thank Dr. Lisa Hall and Dr. Chris Lueth for useful discussions regarding the simulation setup and analysis. Simulations were performed at the National Energy Research Scientific Computing Center, which is supported by the Office of Science of the U.S. Department of Energy under Contract No. DE-AC02-05CH11231. Funding for this work was provided through the Laboratory Directed Research and Development program at Sandia National Laboratories. This work was performed, in part, at the Center for Integrated Nanotechnologies, a U.S. Department of Energy, Office of Basic Energy Sciences user facility. Sandia National Laboratories is a multiprogram laboratory managed and operated by Sandia Corporation, a Lockheed-Martin Company, for the U.S. Department of Energy under Contract No. DE-AC04-94AL85000.

■ REFERENCES

(1) Eisenberg, A.; Kim, J. S. *Introduction to Ionomers*; Wiley-Interscience: New York, 1998.

(2) Schlick, S. *Ionomers: Characterization, Theory, and Applications*; Taylor and Francis, Inc.: New York, 1996.

(3) Baughman, T. W.; Chan, C. D.; Winey, K. I.; Wagener, K. B. *Macromolecules* **2007**, *40*, 6564−6571.

(4) Seitz, M. E.; Chan, C. D.; Opper, K. L.; Baughman, T.; Wagener, K.; Winey, K. I. *J. Am. Chem. Soc.* **2010**, *132*, 8565−8574.

(5) Hall, L. M.; Seitz, M. E.; Winey, K. I.; Opper, K. L.; Wagener, K. B.; Stevens, M. J.; Frischknecht, A. L. *J. Am. Chem. Soc.* **2012**, *134*, 574−587.

(6) Hall, L. M.; Stevens, M. J.; Frischknecht, A. L. *Phys. Rev. Lett.* **2011**, *106*, 127801.

(7) Hall, L. M.; Stevens, M. J.; Frischknecht, A. L. *Macromolecules* **2012**, *45*, 8097−8108.

(8) Yarusso, D. J.; Cooper, S. L. *Macromolecules* **1983**, *16*, 1871−1880.

(9) Kinning, D. J.; Thomas, E. L. *Macromolecules* **1984**, *17*, 1712−1718.

(10) Zhou, N. C.; Chan, C. D.; Winey, K. I. *Macromolecules* **2008**, *41*, 6134−6140.

(11) Winey, K. I.; Laurer, J. H.; Kirkmeyer, B. P. *Macromolecules* **2000**, *33*, 507−513.

(12) Kirkmeyer, B. P.; Tauber, A.; Kim, J.-S.; Winey, K. I. *Macromolecules* **2002**, *35*, 2648−2653.

(13) Kirkmeyer, B. P.; Weiss, R. A.; Winey, K. I. *J. Polym. Sci., Part B: Polym. Phys.* **2001**, *39*, 477−483.

(14) Lin, K.-J.; Maranas, J. *Macromolecules* **2012**, *45*, 6230−6240.

(15) Beers, K. M.; Balsara, N. P. *ACS Macro Lett.* **2012**, *1*, 1155−1160.

(16) Alam, T. M.; Jenkins, J. E.; Bolintineanu, D. S.; Stevens, M. J.; Frischknecht, A. L.; Buitrago, C. F.; Winey, K. I.; Opper, K. L.; Wagener, K. B. *Materials* **2012**, *5*, 1508−1527.

(17) Jorgensen, W. L.; Maxwell, D. S.; Tirado-Rives, J. *J. Am. Chem. Soc.* **1996**, *118*, 11225−11236.

(18) Jensen, K. P.; Jorgensen, W. L. *J. Chem. Theory Comput.* **2006**, *2*, 1499−1509.

(19) Plimpton, S. *J. Comput. Phys.* **1995**, *117*, 1−19.

(20) Hockney, R.; Eastwood, J. *Computer Simulation Using Particles*; Taylor and Francis: New York, 1989.

(21) Waasmaier, D.; Kirfel, A. *Acta Crystallogr.* **1995**, *A51*, 416−431.